Micromachines **2014**, *5*, 275-288; doi:10.3390/mi5020275

OPEN ACCESS

micromachines

ISSN 2072-666X

www.mdpi.com/journal/micromachines

Article

Fabrication of Polydimethylsiloxane Microlenses Utilizing Hydrogel Shrinkage and a Single Molding Step

Bader Aldalali [1,2,*], Aditi Kanhere [1], Jayer Fernandes [1], Chi-Chieh Huang [1] and Hongrui Jiang [1,3,4,5,*]

[1] Department of Electrical and Computer Engineering, University of Wisconsin-Madison, Madison, WI 53707, USA; E-Mails: kanhere@wisc.edu (A.K.); jfernandes@wisc.edu (J.F.); chuang48@wisc.edu (C.-C.H.)

[2] Department of Electrical Engineering, Kuwait University, Khaldiya 13060, Kuwait

[3] Department of Biomedical Engineering, University of Wisconsin-Madison, Madison, WI 53707, USA

[4] Materials Science Program, University of Wisconsin-Madison, Madison, WI 53707, USA

[5] McPherson Eye Research Institute, University of Wisconsin-Madison, Madison, WI 53707, USA

***** Authors to whom correspondence should be addressed; E-Mails: bader.aldalali@ku.edu.kw (B.A.); hongrui@engr.wisc.edu (H.J); Tel.: +965-2498-7380 (B.A.); Fax: +965-2481-7451(B.A); Tel.: +1-608-265-9418 (H.J).

Received: 9 April 2014; in revised form: 9 May 2014 / Accepted: 14 May 2014 / Published: 21 May 2014

Abstract: We report on polydimethlysiloxane (PDMS) microlenses and microlens arrays on flat and curved substrates fabricated via a relatively simple process combining liquid-phase photopolymerization and a single molding step. The mold for the formation of the PDMS lenses is fabricated by photopolymerizing a polyacrylamide (PAAm) pre-hydrogel. The shrinkage of PAAm after its polymerization forms concave lenses. The lenses are then transferred to PDMS by a single step molding to form PDMS microlens array on a flat substrate. The PAAm concave lenses are also transferred to PDMS and another flexible polymer, Solaris, to realize artificial compound eyes. The resultant microlenses and microlens arrays possess good uniformity and optical properties. The focal length of the lenses is inversely proportional to the shrinkage time. The microlens mold can also be rehydrated to change the focal length of the ultimate PDMS microlenses. The spherical aberration is 2.85 μm and the surface roughness is on the order of 204 nm. The microlenses can resolve 10.10 line pairs per mm (lp/mm) and have an f-number range between f/2.9 and f/56.5. For the compound eye, the field of view is 113 °.

Keywords: microlenses; microlens arrays; compound eye; tunable lenses; hydrogels

1. Introduction

The utilization of microlenses has increased dramatically in many different applications including optical communications, imaging, and printing [1]. Due to this demand, different techniques to fabricate microlenses have emerged, including ink-jet printing [2], greyscale lithography [3], and photoresist thermal reflow [1]. The ink-jet printing method uses expensive equipment that requires very precise alignment in order to produce uniform arrays, while greyscale lithography faces difficulty in fitting the desired microlens shape into the different shades of grey [4,5]. In the case of the photoresist reflow method, the lenses are usually used as a mold since they have a high optical absorption under white light and need to be transferred to more optically transparent and stable substrates in a double transfer process [5–7]. There are other approaches that could generate the microlens mold; however, these approaches rely on accurate pressure or temperature control to achieve uniformity among the microlenses [8–10]. These approaches also rely on double transfer for ultimate formation of the microlenses which further elongates and complicates the fabrication process. It is thus highly desirable to develop low-cost, versatile, and simple microlens fabrication methods.

Another appealing feature of microlens arrays that gained popularity recently is their ability to be fabricated onto curved surfaces to increase their field of view (FOV), mimicking the compound eyes of insects [11–15]. Most of the existing fabrication methods rely on ultrafast lasers to fabricate the microlenses, which is very expensive [11,16]. Other methods rely on stress-alleviating bridges between the microlenses, which decreases the fill factor and requires a hard spherical shell under the microlenses to provide the desired curvature [13]. Another available low-cost fabrication method relies on the deformation of the microlens substrate by applying force to provide curvature, which is a very sensitive process and might damage the microlenses [15].

To provide a low-cost, simple fabrication process for microlenses on both planar and curved surfaces, we utilize the capabilities of advanced materials such as hydrogels [17,18]. Due to the high water content, hydrogels could shrink in air as they dry out [17]. We could take advantage of this natural shrinkage property of hydrogels in air to produce smooth concave microlenses and then transfer the microlenses to other more optically transparent and flexible substrates to form convex microlenses using a single molding step.

2. Fabrication

The fabrication process is divided into two segments. The first segment describes the process of fabricating the microlenses by liquid phase photopolymerization and hydrogel shrinkage. The second segment describes the added steps needed to fabricate the artificial compound eye structure using the hydrogel based microlenses.

2.1. Equipment and Materials

All photopolymerization processes were done using a desktop EXFO Acticure 4000 ultra-violet (UV) light source (EXFO Photonic Solutions, Inc, Missisauge, ON, Canada). Photomasks were printed using high-resolution films (3000 dpi, Imagesetter, Inc., Madison, WI, USA).

Two polymers were used to fabricate the microlens mold. A photopolymerizable prepolymer, isobornyl acrylate (IBA), made as per the recipe found in [19] was used as the structure that defines the microlens apertures. The other polymer is a photopolymerizable polyacrylamide (PAAm) based pre-hydrogel. The PAAm pre-hydrogel solution included a monomer, crosslinker, photoinitiator, and water as a solvent and was made as per the recipe in [20]. The PAAm was used as the mold for the microlenses. PDMS (Sylgard 184, Dow Corning Corporation, Midland, MI, USA) was used as the microlens material.

For the compound eye structure, in addition to PDMS, another polymer called Solaris (Smooth-on, Easton, PA, USA) was used as an alternative for the substrate of the compound eye. Solaris is a transparent silicone polymer which is widely used as a protective layer on top of solar cells [21].

2.2. Microlens Array Fabrication

Figure 1 shows fabricated PDMS microlenses with 0.7-mm diameter (called hereafter 0.7-mm microlenses).The fabrication process is shown in Figure 2. A polycarbonate cartridge well (40-mm × 22-mm × 0.36-mm, HybriWells, Grace Bio-Labs Inc., Bend, OR, USA) was utilized to define the apertures of the microlenses. The cartridge well consisted of two top and bottom plates connected by a 360-μm-thick adhesive spacer which defined the depth of the well. The bottom surface was first peeled off and the remaining surface with the spacer was placed onto a plastic slide. IBA was flowed into the well using a transfer pipette. The prepolymer IBA was then exposed to ultraviolet (UV) light at 10 mW/cm^2 for 25s with a mask defining the microlens apertures. Photopolymerizable IBA acts as a negative photoresist when exposed to UV light. After exposure, the top plate was peeled off and unpolymerized IBA was rinsed away with ethanol.

Figure 1. (**a**) Optical image of a 0.7-mm microlens array. (**b**) Scanning electron microscopy image of 0.7-mm microlens.

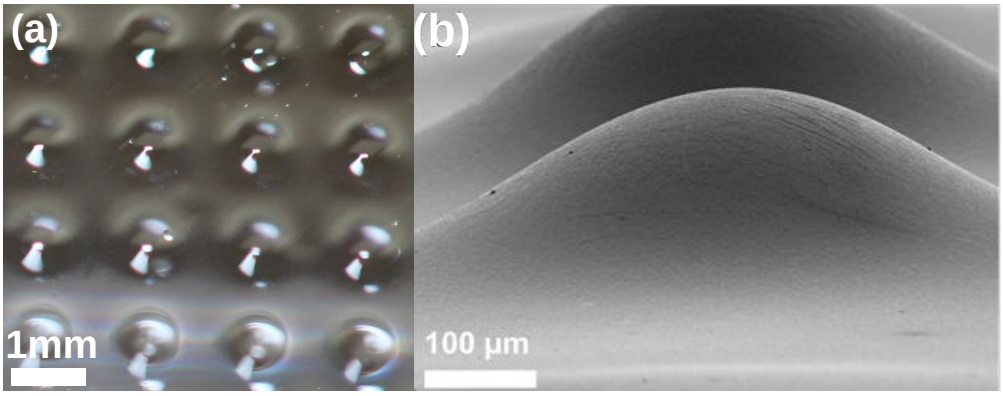

Figure 2. Fabrication process of the polydimethlysiloxane (PDMS) microlenses by hydrogel shrinkage. (**a**) Isobornyl acrylate (IBA) prepolymer was flowed into the cartridge and exposed under ultraviolet light. The IBA was flowed using a pipette until it filled the chamber. The IBA was exposed at 10-mW/cm^2 for 25 s. (**b**) Top plastic plate is peeled off exposing the patterned aperture array and uncured IBA was washed away using ethanol. The top surface and sidewalls of the aperture array were treated with oxygen plasma. (**c**) Treated structure was flipped onto a glass slide with a 250–300 μm spacer. (**d**) Photopolymerizable polyacrylamide (PAAm) based pre-hydrogel is flowed into the chamber and allowed to fill the whole aperture array including the top surface. (**e**) The PAAm is allowed to dry in air for 24 h. The PAAm will shrink through the apertures and be pinned at the hydrophobic-hydrophilic boundary. (**f**) The microlens mold is then treated with octadecyltrichlorosilane to decrease the adhesion of PDMS to the mold. (**g**) Uncured PDMS is then flowed on top of the mold and allowed to cure. (**h**) Cured PDMS is then peeled off. (**I**) The final PDMS microlens array.

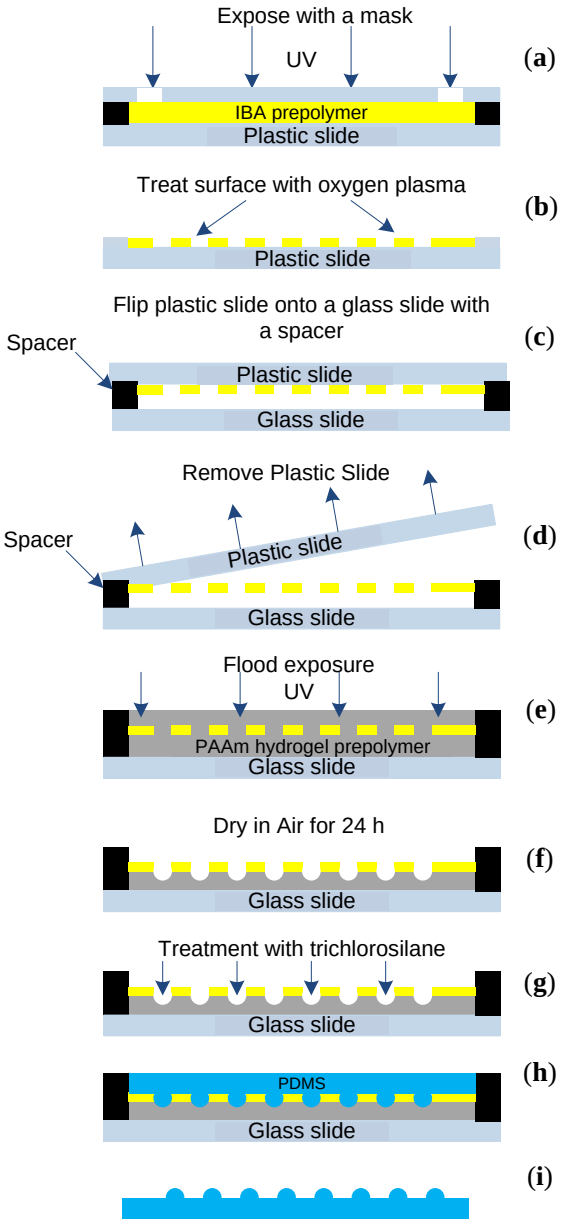

At this point, the structure included a polymerized IBA (poly-IBA) surface with an array of apertures on top of a plastic slide as in Figure 2b. The surface of the poly-IBA was then treated with oxygen plasma by a reactive ion etching RIE system (Unaxis 790, Unaxis Wafer Processing, Schwyz, Switzerland) using the following parameters: power supply = 100 W, treatment time between 30 s and 3 min. Oxygen plasma only rendered the top surface and sidewalls of the poly-IBA hydrophilic since the bottom surface was attached to the plastic slide and hence protected from the plasma. A hydrophobic-hydrophilic boundary was created between the bottom surface of the poly-IBA and the remaining structure, which was utilized to form the microlenses. A double-sided adhesive (250–300 μm thick) was added to a glass slide to define a chamber. The plastic slide along with the poly-IBA, was then flipped onto the glass slide. The plastic slide was peeled off as can be seen in Figure 2c.

At this step, the structure consisted of an array of poly-IBA apertures on top of a 280-μm-high chamber. Epoxy was then applied around the boundary of the structure to prevent any leakage. Using a syringe, a photopolymerizable polyacrylamide (PAAm) based pre-hydrogel was then flowed through one of the holes and was allowed to fill the chamber as well as the top surface of the poly-IBA as in Figure 2d. The PAAm pre-hydrogel was then flood exposed under UV light at 25 mW/cm^2 for 90 s. The PAAm hydrogel was then allowed to dry in air for 24 h.

After exposure, the PAAm hydrogel shrunk in air due to the high water content. In this solution, PAAm contained 85% water. In similar solutions, with 80% water, PAAm shrunk to 36% of its initial volume [17]. The hydrogel shrunk until it reached the top surface of the poly-IBA apertures where it was pinned at the boundary of the hydrophobic top surface and the hydrophilic sidewall. This resulted in a concave lens as shown in Figure 2e. Figure 3 shows the PAAm before and after shrinking. The PAAm substrate was placed on top of an array of the letter "W" and images were taken using the stereoscope. In Figure 3a, the PAAm fully covers the aperture array and hence no lenses have formed. In Figure 3b, the PAAm has started to shrink and has formed a concave lens at the boundary of the apertures. An erect minified image "W" can be seen below the aperture array.

A key parameter during the fabrication process is the initial amount of PAAm pre-hydrogel. If too little PAAm is flowed, the hydrogel will shrink into the chamber, and if too much is flowed, the hydrogel will not reach the top poly-IBA aperture surface. PAAm should also be flowed uniformly on top of the aperture array to ensure uniform shrinking and eventually more uniform microlens arrays. However, since the top surface of the poly-IBA has been treated to make it hydrophobic, the PAAm that flows on top of the aperture array would tend to combine together and form a bubble-like profile. To overcome that, the PAAm pre-hydrogel was overflowed until it formed a relatively flat layer on top of the aperture array.

After 24 h, the PAAm surface was then treated with octadecyltrichlorosilane (OTS) in a vacuum for an hour rendering it even more hydrophobic [22]. After the OTS treatment, PDMS prepolymer mixed with the curing agent at a weight ratio of 10:1 was also placed in vacuum for an hour and then poured over the PAAm surface. The PDMS was then cured at 70 °C overnight and then peeled off.

Figure 3. Images of the PAAm hydrogel on top of the poly-IBA. (**a**) Shows the PAAm right after exposure and before shrinking. (**b**) Shows clear images of "W" under the poly-IBA apertures. The images are erect, minified and are visible between the object plane and the aperture array, hence concave lenses.

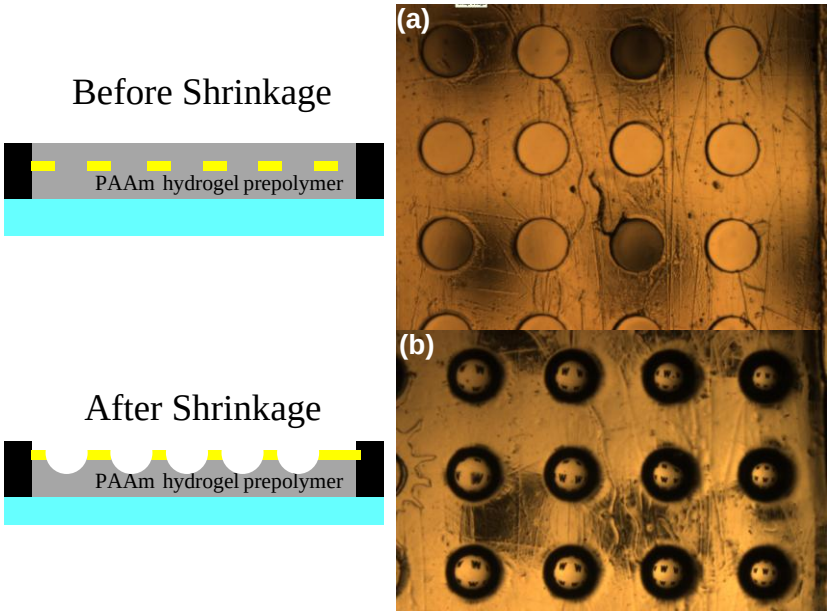

2.3. PDMS Compound Eye Fabrication

Figure 4 shows the added steps required to fabricate the compound eye structure. The fabrication process was inspired by the hemispherical camera work in [14]. PDMS was flowed on top of a plastic hemispherical shell with a 1.1-cm diameter. After curing, the PDMS was peeled off and placed on top of a cork with a diameter of 1.5-cm as in Figure 4b.The PDMS was then stretched from four opposite directions to realize a flat PDMS surface on top of the cork. On the other end, uncured PDMS was placed on top of a hydrogel microlens mold that has been allowed to shrink for at least 24 h. This minimum time requirement allows the PDMS to be easily peeled off later on in the fabrication process. The flattened PDMS and cork structure was then flipped onto the uncured PDMS and allowed to contact. It was very important to maintain a very thin layer of PDMS on top of the mold since a thick layer of PDMS will deform the hemispherical structure. The whole cork and mold structure was then placed in the oven at 75 ℃ to cure overnight. After the PDMS was cured, the whole structure was carefully peeled away from the hydrogel mold and the adhesive tape was then removed to allow the PDMS to retain its original shape.

2.4. Solaris Compound Eye Fabrication

We later substituted PDMS with Solaris to achieve a higher FOV. Solaris can be elongated to a length of 290% before breakage, which allows for utilizing most of the hemisphere [21]. In the same manner as PDMS, Solaris was cured by mixing the Solaris pre-polymer with the curing agent in a weight ratio of 1:1. Using a pipette, small volumes of uncured Solaris were dropped onto the hemispherical shell. Solaris was then cured on a hotplate at 80 ℃ for 10 min.

The trade-off with using Solaris is that the substrate became much softer compared to PDMS. This means that any excessive weight on the substrate will cause it to deform and not retain its spherical shape when it is finally released. In order to strengthen the Solaris structure, after curing the Solaris and removing it from the hotplate, another layer of uncured Solaris was placed on the first layer and cured again on the hotplate for 10 min. After the two-layered Solaris hemispherical substrate was cured, the rest of the fabrication process of Figure 4b–d was followed to produce the compound eye structure. The only other variation to the fabrication process of Figure 4 was that a larger cork was used (diameter = 1.8 cm).

Figure 4. Fabrication process of compound eye. (**a**) Uncured PDMS is flowed on top of plastic hemispherical shell and allowed to cure. (**b**) PDMS hemisphere is placed on top of the cork and stretched until it matches the diameter of the cork. (**c**) Uncured PDMS is placed on top of the hydrogel mold fabricated in Figure 2. Stretched PDMS on top of the cork is then flipped on top of the hydrogel mold. (**d**) Cured PDMS is peeled off from hydrogel mold. The cork is removed which released the stretched PDMS into its original hemispherical shape.

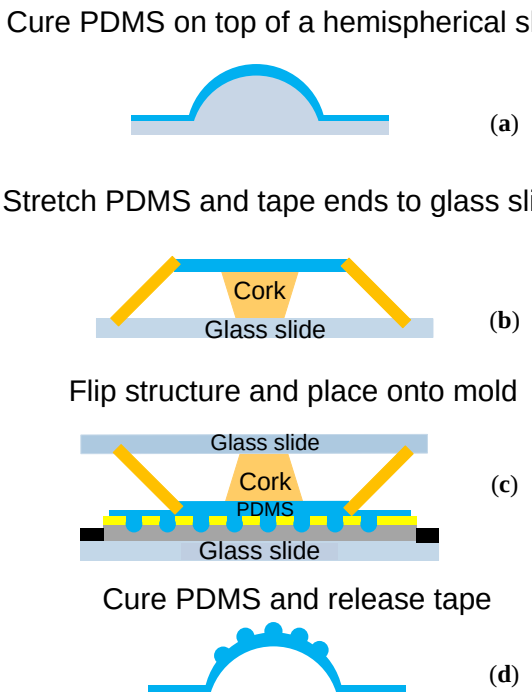

3. Results and Discussion

3.1. Microlens Analysis

Figure 5 shows the three dimensional profile of the 0.7-mm microlens using the white light interferometer (Zygo New View 6300).The microlenses were sputtered with a thin layer of reflective metal (gold or aluminum) prior to being placed under the interferometer to make the surface more reflective. The metal only alters the surface roughness of the microlenses and not the profile [8].As can be seen from Figure 5, the profile is of a 0.7-mm microlens with a height of approximately 31 μmother profile shows good uniformity of curvature across the entire microlens surface.

Figure 5. Three-dimensional profile of the 0.7-mm PDMS microlenses. The profile is taken using a ZYGO white light interferometer. The curvature is uniform across the surface of the microlens.

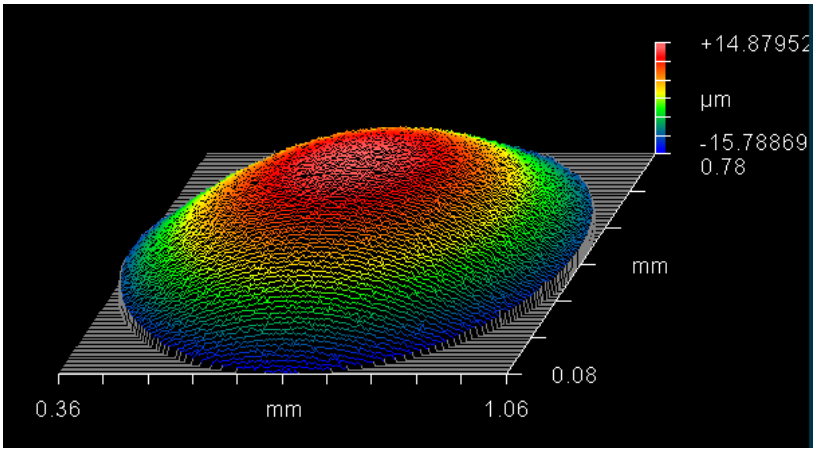

3.2. Image Analysis

The fabrication process can also be used to produce uniform microlens arrays. Figure 6 shows an image of an array of inverted "W"s using a stereoscope and imaged through a 2 × 4 0.7-mm microlens array. As can be seen from Figure 6, the image of the "W"s is clear and sharp for all eight microlenses. The largest percent difference of focal length between four neighboring microlenses is 2.59%. Figure 7 shows images acquired by the PDMS microlenses. In Figure 7a, a 0.7-mm microlens was used to image an inverted "UW". In Figure7b, the United States Air Force (USAF) 1951 resolution test chart was used to determine the resolution of a 0.7-mm microlens. Table 1 shows the resulting optical properties of the microlenses in different sizes. The microlenses can be fabricated with f-numbers varying from f/2.9 to f/56.5.

Figure 6. Image of an array of inverted "W"s imaged through a 2 × 4 microlens array. The eight inverted images are clear and sharp which shows good uniformity among the neighboring microlenses.

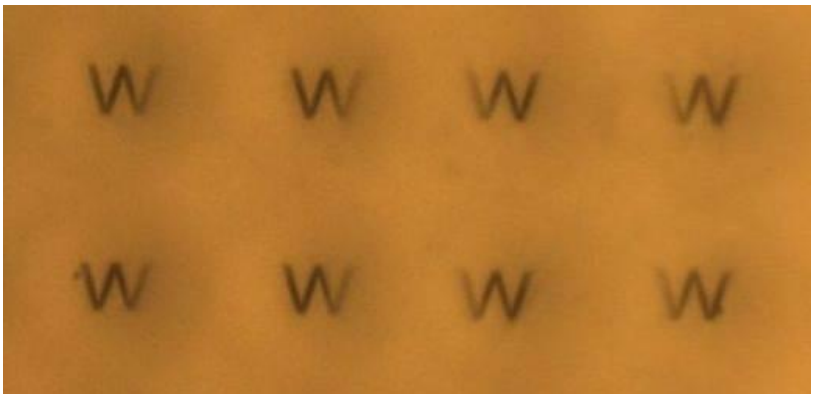

Figure 7. Images under the 0.7-mm PDMS microlenses. (**a**) Shows an image of an inverted "UW" under a 0.7-mm microlens. (**b**) Shows an image of the USAF1951 resolution test chart under a 0.7-mm microlens. The microlens can resolve lines in group 3, element 2.

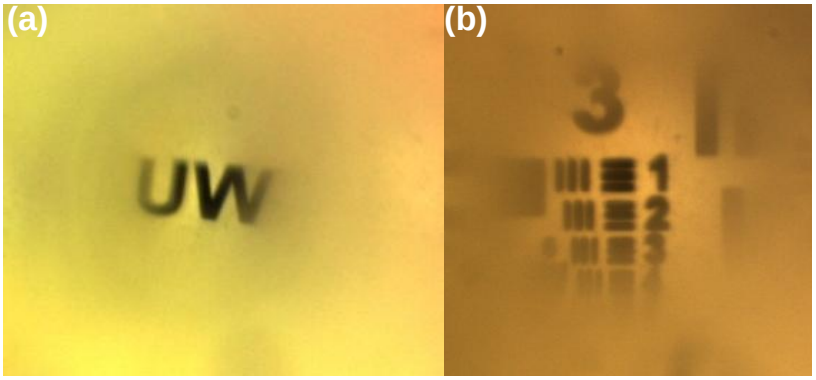

Table 1. Optical properties of PDMS microlenses with different sized apertures.

Parameter	0.7-mm	1-mm
Focal length (mm)	5.417	2.94
Spherical aberration (μm)	2.85	31.276
Resolution (lp/mm)	8.98	7.13
Roughness (nm)	204	320

Table2. Optical properties of PDMS microlenses with different shrinkage times.

Parameter	Shrinkage (h)			
	9	12	18	24
Focal length (mm)	39.57	16.2	11.55	5.63
Spherical aberration (μm)	0.634	2.147	3.59	9.66
Roughness (nm)	110	204	255	187

3.3. Shrinkage

The relationship between hydrogel shrinkage and resultant optical properties has also been studied. Table 2 shows the resulting optical properties for 0.7-mm microlens arrays that were allowed to shrink for different durations before PDMS molding. The arrays included 5 × 7 microlenses and the size of the overall array was 2 × 1 call the arrays had an initial PAAm pre-hydrogel volume of 1ml prior to photopolymerization. The shortest duration as can be seen from Table 2 is 9 h. Shorter shrinkage times resulted in the PDMS sticking to the substrate and preventing it from being peeled off. This was due to the high water content still present in the hydrogel. It should be noted that both uniformity and yield increased with shrinkage time, especially between 9 and 12 h.

It can be seen from Table 2 that as the shrinkage time is increased, the focal length decreases, while both the spherical aberration and the surface roughness increases. The increase in surface roughness is due to the loss of water in the hydrogel as it shrinks. The increase in focal length is due to the fact that as the shrinking time increases the hydrogel shrinks down further through the aperture which increases both the height and curvature of the PDMS microlens. The height of the microlens and the focal length are related by the following two equations [23,24]:

$$R = \frac{h^2 + \left(\frac{d}{2}\right)^2}{2h} \quad (1)$$

and

$$f = \frac{R}{n-1} \quad (2)$$

where R is the radius of curvature of the microlens, h is the height, d is the diameter, and n is the refractive index which in the case of PDMS is 1.43 [25].

3.4. Rehydration

After the PDMS has been peeled off the mold, the mold can still be utilized to produce microlenses with different focal lengths than the original mold. This is achieved by rehydrating the mold with water. Rehydrating the mold allowed the hydrogel to swell up and produce a new curvature. The mold was then allowed to shrink and PDMS was then poured and cured on the rehydrated mold. Using the same mold, we measured three different samples of 1-mm microlenses that were hydrated to different levels. Between the three samples, the focal length varied from 4.4 mm to 20.59 mm. The surface roughness also varied from 686 nm to 195 nm. This capability allows control over the focal length and surface requirement even after the microlens mold is fabricated.

3.5. Compound Eye

Figure 8 shows the compound eye structure on a hemispherical shell which was fabricated as per Figure 4. The initial compound eye structure as can be seen from Figure 8 is made from PDMS. The FOV achieved by the PDMS compound eye is ~94 °. As per the fabrication process in Figure 4, the FOV is dependent on how much the PDMS substrate can be stretched from a sphere onto a flat surface. Theoretically, the PDMS can be elongated before breaking to 156% of its original size [26]. Note that the images in Figure 8c–d are taken using a stereoscope where an array of the letters “UW” are placed under the compound eye and on top of the light source of the stereoscope. The focus is then adjusted until it reaches the focal distance of some of the microlenses of the compound eye

The FOV achieved by the Solaris compound eye is ~113 º. The FOV for both the PDMS and Solaris compound eye was calculated by placing a laser source at the periphery of a rotational stage (RBB12, Thorlabs Inc, Newton, NJ, USA) and placing the compound eye in the middle of the stage. The laser was aligned with a microlens at one end of the compound eye. The laser was then rotated across a line of microlenses and the FOV was equivalent to the rotation angle from the first focused spot to the last focused spot of the line of microlenses. When the laser passes through the microlens, the spot size should converge into a focal spot; however, in this case due to the small size of the microlenses and the laser beam, the focal spot was hard to observe. We therefore looked instead at the far-field diffraction pattern. If the far-field diffraction pattern was an Airy disk, then the laser source is aligned with one of the microlenses. If any other pattern is visible, then the laser beam is either between the microlenses or outside the FOV.

Figure 8. Artificial compound eye. (**a**) PDMS compound eye with 0.7-mm microlenses. Field of view achieved by the compound eye is 94°. (**b**) Solaris compound eye with 0.7-mm microlenses. Field of view achieved by the compound eye is 113°. (**c**) Images acquired by PDMS compound eye. (**d**) Images acquired by Solaris compound eye.

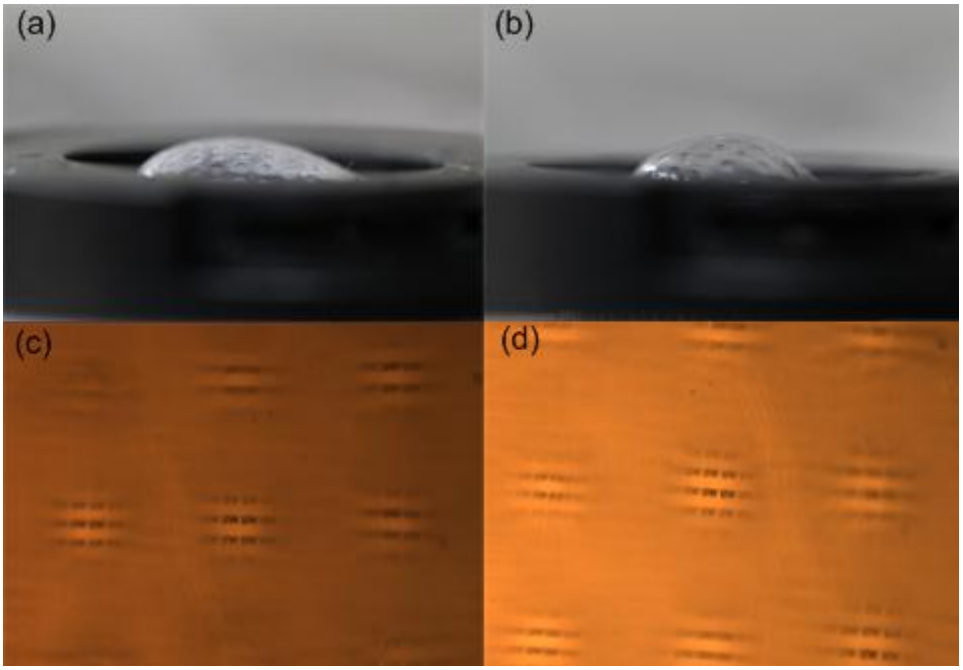

3.6. Aperture Limitation

It should be noted that there is an upper limit on the aperture size that can be achieved using the hydrogel shrinkage fabrication process. The main reason behind the limitation is due to the fact that as the aperture size increases, surface tension forces which are necessary for forming the required microlens profile become far less dominant when compared to the gravitational forces which become more dominant as the aperture size is increased [27]. Also in this case, gravitational forces would have a bigger impact compared to other fabrication techniques since we are fabricating concave lenses with profiles that are curved towards the gravitational force and not against it.

3.7. Time Sensitive Fabrication Process

When treating the surface of the IBA hydrophilic to create a hydrophobic and hydrophilic boundary, it should be noted that it is only a temporary process and the substrate will recover its natural hydrophobic state with time [9]. That means that the PAAm surface has to be flowed into the IBA chamber within hours after treatment or the surface will reverse into its original hydrophobic status. If the PAAm is flowed within the allocated time slot and exposed, the polymerized hydrogel will retain the lens curvature and is not time sensitive anymore.

4. Conclusions

We demonstrated PDMS microlenses and uniform microlens arrays fabricated through shrinking of a hydrogel and a single transfer step. The microlenses can be fabricated with lesser control

requirements and can provide a wide range of f-numbers. The resulting aberrations are minimal for the small microlenses but increase with increasing apertures. Focal length is inversely proportional to the shrinkage time of the hydrogel while spherical aberration and surface roughness are directly proportional to the shrinkage time. The hydrogel mold can be rehydrated to produce microlenses with different focal lengths. An artificial compound eye based on the hydrogel shrinkage microlenses has also been demonstrated using two kinds of flexible polymers. Future work will focus on increasing the field of view of the compound eye as well as coupling microlenses with charge-coupled devices to produce complete optical system. Work will also include study of the correlation between the IBA mask size and the aperture size and shape of the resulting microlenses. In addition, work will include researching polymers that are more robust than PDMS to sustain long-term use.

Acknowledgments

The authors thank C. Li for technical discussions and help. This research utilizes National Science Foundation supported facilities at the University of Wisconsin. This work was supported by the U.S. National Science Foundation through the Emerging Frontiers in Research and Innovation program (EFRI 0937847). The work of the first author was supported by Kuwait University through its graduate student scholarship program.

Author Contributions

B. Aldalali performed most of the fabrication, analysis, and wrote the manuscript. A. Kanhere worked on the experiments pertaining to the hydrogel mold and planar PDMS microlenses. C. Huang performed the oxygen plasma processes, the PDMS compound eye, as well as the SEM images. J. Fernandes worked on both the Solaris and PDMS compound eye and on the analysis of the microlenses. H. Jiang had overall oversight over the experiments and manuscript writing.

Conflicts of Interest

The authors declare no conflict of interest.

References

1. Yang, H.; Chao, C.-K.; Wei, M.-K.; Lin, C.-P. High fill-factor microlens array mold insert fabrication using a thermal reflow process. *J. Micromech. Microeng.* **2004**, *14*, 1197–1204.
2. Beihl, S.; Danzebrikn, R.; Oliveira, P.; Aegerter, M.A. Refractive microlens fabrication by ink jet process. *J. Sol-Gel Sci. Technol.* **1998**, *13*, 177–182.
3. Rogers, J.D.; Karkkainen, A.H.O.; Tkaczyk, T.; Rantala, J.T.; Descour, M.R. Realization of refractive microoptics through grayscale lithographic patterning of photosensitive hybrid glass. *Opt. Express* **2004**, *12*, 1294–1303.
4. Yu, X.; Wang, Z.; Han, Y. Microlenses fabricated by discontinuous dewetting and soft lithography. *Microelectron. Eng.* **2008**, *85*, 1878–1881.
5. Huang, L.-C.; Lin, T.-C.; Huang, C.-C.; Chao, C.-Y. Photopolymerized self-assembly microlens arrays based on phase separation. *Soft Matter* **2011**, *7*, 2812–2816.

6. Daly, D. *Microlens Arrays*; Taylor and Francis: New York, NY, USA, 2001.
7. Park, S.; Jeong, Y.; Kim, J.; Choi, K.; Kim, H.C.; Chung, D.S.; Chun, K. Fabricaton of poly(dimethylsiloxane) microlens for laser-induced fluorescence detection. *Jpn. J. Appl. Phys. Part 1 Regul. Pap. Short Notes Rev. Pap.* **2006**, *45*, 5614–5617.
8. Zeng, X.; Jiang, H. Polydimethylsiloxane microlens arrays fabricated through liquid-phase photopolymerization and molding. *J. Microelectromech. Syst.* **2008**, *17*, 1210–1217.
9. Kim, H.-K.; Yun, K.-S. Fabrication of PDMS Microlenses with Various Curvatures Using a Water-Based Molding Method. In Proceedings of the 12th International Conference on Miniaturized Systems for Chemistry and Life, San Diego, CA, USA, 12–16 October 2008; pp. 994–996.
10. Yu, H.; Zhou, G.; Chau, F.S.; Lee, F. Fabrication and characterization of PDMS microlenses based on elastomeric molding technology. *Opt. Lett.* **2009**, *34*, 3454–3456.
11. Qu, P.; Chen, F.; Liu, H.; Yang, Q.; Lu, J.; Si, J.; Wang, Y.; Hou, X. A simple route to fabricate artificial compound eye structures. *Opt. Express* **2012**, *20*, 5775–5782.
12. Jeong, K.-H.; Kim, J.; Lee, L.P. Biologically inspired artificial compound eyes. *Science* **2006**, *312*, 557–561.
13. Zhu, D.; Zeng, X.; Li, C.; Jiang, H. Focus-tunable microlens arrays fabricated on spherical surfaces. *J. Microelectromech. Syst.* **2011**, *20*, 389–395.
14. Ko, H.C.; Stoykovich, M.P.; Song, J.; Malyarchuk, V.; Choi, W.M.; Yu, C.-J.; Geddes, J.B., III; Xiao, J.; Wang, S.; Huang, Y.; Rogers, J.A. A hemispherical electronic eye camera based on compressible silicon optoelectronics. *Nature* **2008**, *454*, 748–753.
15. He, Q.; Liu, J.; Yang, B.; Dong, Y.; Yang, C. Fabrication and characterization of biologically inspired curved-surface artificial compound eyes. *J. Microelectromech. Syst.* **2013**, *22*, 4–6.
16. Radtke, D.; Duparré, J.; Zeitner, U.D.; Tünnermann, A. Laser lithographic fabrication and characterization of a spherical artificial compound eye. *Opt. Express* **2007**, *15*, 3067–3077.
17. Das, A.L.; Mukherjee, R.; Katiyer, V.; Kulkarni, M.; Ghatak, A.; Sharma, A. Generation of sub-micrometer-scale patterns by successive miniaturization using hydrogels. *Adv. Mater.* **2007**, *19*, 1943–1946.
18. Dong, L.; Agarwal, A.K.; Beebe, D.J.; Jiang, H. Adaptive liquid microlenses activated by stimuli-responsive hydrogels. *Nature* **2006**, *442*, 551–554.
19. Agarwal, A.K.; Beebe, D.J.; Jiang, H. Integration of polymer and metal microstructures using liquid-phase photopolymerization. *J. Micromech. Microeng.* **2006**, *16*, 332–340.
20. Sridharamurthy, S.S.; Dong, L.; Jiang, H. A microfluidic chemical/biological sensing system based on membrane dissolution and optical absorption. *Meas. Sci. Technol.* **2007**, *18*, 201–207.
21. Smooth-on Corp Homepage. Available online: http://www.smooth-on.com (accessed on Day Month Year).
22. Aldalali, B.; Zhu, D.; Jiang, H. Fabrication of Polydimethylsiloxane Microlens Arrays on Curved Surfaces. In Proceedings of the 16th International Conference on Optical MEMS and Nanophotonics Istanbul, Istanbul, Turkey, 2011; pp. 239–240.
23. Zappe, H. Micro-optics: A micro-tutorial. *Adv. Opt. Technol.* **2012**, *1*, 117–126.
24. Nussbaum, P.; Volkel, R.; Herzig, H.P.; Eisner, M.; Haselbeck, S. Design, fabrication and testing of microlens arrays for sensors and microsystems. *Pure Appl. Opt.* **1997**, *6*, 617–636.

25. Chang-Yen, D.A.; Eich, R.K.; Gale, B.K. A monolithic PDMS waveguide system fabricated using soft-lithography techniques. *J. Lightwave Technol.* **2005**, *23*, 2088–2093.
26. Huang, N.; Lee, R.; Li, S. Engineering of aligned skeletal muscle by micropatterning. *Am. J. Transl. Res.* **2010**, *2*, 43–55.
27. Zeng, X.; Jiang, H. *Microlenses: Properties, Fabrication and Liquid Lenses*; Taylor and Francis: Boca Raton, FL, USA, 2013.